

58000098

Lund-MPh-80/09

ON THE INTERACTION BETWEEN THE GROUND- AND  
S-BANDS IN THE CHFB MODEL

H.-B. HAKANSSON



LUND INSTITUTE OF TECHNOLOGY

Department of Mathematical Physics

ON THE INTERACTION BETWEEN THE GROUND- AND  
S-BANDS IN THE CHFB MODEL

H.-B. Håkansson  
Department of Mathematical Physics  
Lund Institute of Technology  
Box 725  
S-220 07 Lund, Sweden

Abstract. The interaction between the ground configuration and the first excited 2 qp (s-) configuration in the  $i_{13/2}$  CHFB model is eliminated in order to investigate how the interaction is built up by the different terms in the Hamiltonian. The changes of sign of the interaction can be understood from the particle number projected wave functions. Oscillations are still present after projection.

It has become apparent that the cranked Hartree-Fock-Bogoliubov (CHFB) method provides a powerful tool for studying high spin states in nuclei, see e.g. the review articles by Goodman [1] and Faessler et al. [2]. It should be noted, though, that the method unfortunately has some less appealing aspects, such as the large spread in particle number and angular momentum especially in the band crossing region [3,4]. An interesting feature of the model is the oscillating character of the interaction strength between the zero quasiparticle (0 qp- or ground-) configuration and the first excited 2 qp (Stockholm) configuration as a function of the chemical potential,  $\lambda$ , within a high-j shell. This feature was first noticed by Bengtsson et al. [5] in 1978 and since then it has been much discussed. These oscillations appear in the particle-rotor model [6,7] as well as in the CHFB model and seem to be present also in experimental data. It has been alleged that the variations in the degree of backbending of the Yb isotopes is an experimental confirmation of the oscillations. These ideas have made a wide appeal [2,5,9] especially since there are indications of similar qualitative behaviours also in other cases, e.g. for the  $h_{11/2}$  protons in the N=90 isotones.

In this note we have used the  $i_{13/2}$  cranking model of Hamamoto [3,8] to investigate the character of the interaction between the yrast and yrare bands before and after particle number projections. (Henceforth this interaction may occasionally be referred to as just the interaction.) This model is, despite its simplicity, enough structured and realistic to make investigations of this kind meaningful. By applying an exact and algebraic number projection technique we have been able to understand the mechanism behind the changes of sign of the interaction.

The cranking Hamiltonian is

$$H = H_{sp} - \lambda \hat{N} - \omega j_x - \Delta(P^\dagger + P) \quad (1)$$

where

$$H_{sp} = \kappa [3m^2 - j(j+1)] / [j(j+1)] + e_0 \quad (2)$$

and the parameters  $\kappa$ ,  $\Delta$ ,  $e_0$  are 0.392, 0.12, 6.655 respectively, all in units of  $M\omega_0$ . In cases where expectation values and matrix elements are calculated between states of well-defined particle number we have used the pairing force  $GP^\dagger P$  instead of the pair field  $\Delta(P^\dagger + P)$ . The above parameter values are chosen so as to be realistic in the rare-earth region. A larger  $\Delta$ -value would, however, facilitate the calculations considerably by making the crossings more distinct and thus easier to determine accurately.

The nature of the interaction matrix-element between the ground- and the s-configurations is of course highly dependent on what is defined as interaction-free configurations. We define them as those forming strictly straight lines in a quasiparticle energy diagram [9] at the crossing, i.e. we require that they should have constant expectation values of  $j_x$ . By this definition the wavefunction of a certain configuration will change only insignificantly when  $\omega$  passes the crossing frequency,  $\omega_c$ . This is, we think, an obvious property of a non-perturbed configuration. It is in general possible to eliminate not only the interaction at the first "crossing" but also those at the following two or three "crossings" [8]. In certain situations, however, it can be very hard to find the critical frequency  $\omega_c$  and one may be forced to enclose the proper value of  $\omega_c$  by testing the wave functions (e.g. by calculating  $\langle j_x \rangle$ ) for a large number of  $\omega$ -values. In cases when two or more crossings merge the elimination will fail [4], but such situations are fortunately rare.

In the approach of ref. [5] the term  $\omega j_x$  of the Hamiltonian is claimed to represent the interaction. This requires, however, a specific definition of the non-interacting configurations, very different from ours as can be understood from fig. 1. In the upper part of this figure we have plotted the matrix elements of  $H$  (solid),  $H_{sp}$  (dashed) and  $\Delta(P^\dagger+P)$  (dotted) between the non-interacting ground and Stockholm configurations. We see that  $\langle H_{sp} \rangle$  is always the largest quantity while  $\langle \omega j_x \rangle$  is very small and not depicted in the figure. We also see that  $\langle H_{sp} \rangle$  and  $\langle P^\dagger+P \rangle$  oscillate more or less in phase and that they, with proper signs chosen, sum up almost exactly to  $V (= \langle H \rangle)$  which is half of the energy difference between the two interacting levels at the crossing frequency ( $\omega_c$ ). It is not surprising that  $\omega j_x$  has such a small matrix element between the two non-interacting levels as the expectation values of  $j_x$  for these levels generally differs with more than ten units in the crossing region. However, each individual term in the Hamiltonian couples as a rule to other adjacent levels, and this explains why  $\langle P^\dagger+P \rangle$  is still so large although  $[j_x, P^\dagger] = [j_x, P] = 0$ .

The two solid lines in fig. 1, marked with N, which cross each other five times describe the expectation values of the number operator for the ground-state wave function (vacuum) and the first excited 2 qp wave functions at  $\omega = \omega_c$  before the interaction has been eliminated. The curves represent the combination of two discontinuous lines which interchange

character and make jumps five times approximately halfway between the crossings. It is worthwhile noting that these crossings coincide with even particle numbers ( $i$ ), and that the corresponding  $\lambda$ -values ( $\lambda_i$ ) fall exactly at the maxima of the interaction matrix elements. Thus a definite even particle number can be assigned to every interaction peak, i.e. we have the two-, four-, six-particle peaks etc.

We resolve the wave-functions of the non-interacting configurations ( $g$  and  $s$ ) into components having well-defined particle-number:

$$\psi^g(\lambda, \omega_c) = \sum_n \phi_n^g(\lambda, \omega_c) \quad n = 0, 2, \dots, 14 \quad (3)$$

$$\psi^s(\lambda, \omega_c) = \sum_n \phi_n^s(\lambda, \omega_c). \quad n = 0, 2, \dots, 14 \quad (4)$$

In the lower part of fig. 1 we have plotted  $P_n^g = |\phi_n^g(\lambda, \omega_c)|^2$  (solid curves) and  $P_n^s = |\phi_n^s(\lambda, \omega_c)|^2$  (dashed curves). A closer inspection shows that the product  $P_i^g \cdot P_i^s$  is at its maximum for  $\lambda = \lambda_i$ , a fact which further accentuates the association of the interaction peaks with definite even particle numbers. If in this model we only allow even particle numbers, i.e. we consider only the corresponding parameter values  $\lambda_i, \omega_{ci}$ , then the interaction strength as a function of  $n$  behaves as indicated by the dots in fig. 1 which reminds very much of the results of the particle number conserving calculations of ref. [10].

If all single-particle energies are set equal ( $\kappa=0$ ) there will be no interactions at all. Every qp-energy will be a linear function of  $\omega$  and only sharp crossings arise. On the other hand, in the representation of ref. [7] the interaction is attributed to the linearized pairing force active between states of particle numbers differing by two units. This limit is to some extent also inherent in the CHFB-model, because if  $\Delta$  goes to zero and the excited 2 qp-state at the same time goes over into a state of particle number differing by two units\* from the ground-state no interaction can occur. Consequently, the interaction between the two lowest configurations in the CHFB-model depends critically on the pair field, although  $H_{sp}$  dominates when the non-interacting configurations are defined as above. As we shall see, an inspection of the number projected wave functions furnishes further insight into the strange oscillations.

\* This is normally the case when  $\lambda$  is kept constant.

When the non-interacting g- and s-configurations are established we can use them as normal CHFB vacua, i.e. we can transform the wave functions into the canonical basis [11] and perform a particle number projection. We use an algebraic projection technique [8] which generates wave functions in terms of uncoupled Slater determinants; the m-scheme representation. This procedure facilitates the subsequent calculations considerably and all matrix elements, expectation values etc. are easily evaluated.

As the parameter values of the two configurations are identical, the scalar product between  $\psi^g$  and  $\psi^s$  ((3) and (4)) will be zero, i.e.

$$\langle \psi^g | \psi^s \rangle (\lambda, \omega_c) = \sum_n \langle \phi_n^g | \phi_n^s \rangle (\lambda, \omega_c) = 0. \quad (5)$$

In figure 2 we have drawn with solid lines these overlap components as a function of  $\lambda$ . We see that every second overlap function has their main peaks positive while the others are negative. It is obvious that this is the only possible combination of phases that can give the result of eq. (5). As a matter of fact, the phases come automatically from the calculations and are thus inherent in the model and its wave functions. These changes of sign may give us a hint of the mechanisms behind the oscillation (i.e. sign changes) of the interaction whose absolute value are depicted in fig. 1. It is not surprising that also other matrix elements than that of the unit operator behave in a similar manner, see the dashed lines of fig. 2.

In fig. 2 we have marked with downwards pointing arrows those  $\lambda$ -values where we have no interactions in the original wave functions and with upward-directed arrows those  $\lambda$ -values giving maximal interaction, see fig. 1. As now the matrix elements of e.g.  $H_{sp}$  more or less follow the overlap functions (see fig. 2) we can understand the cancellations as being due to a competition between the contributions from two different particle numbers  $n$  and  $n+2$ . The arrows pointing up stand where the overlaps of particle numbers  $n+2$  and  $n-2$  are of equal magnitude and where their product has a minimum. This results in the domination of the  $n$ -particle contribution. Furthermore, at these  $\lambda$ -values the product of the  $n$ -particle norms are also maximal as shown in the lower part of fig. 1.

In fig. 2 we see that every overlap function changes sign before it vanishes. Through a magnifying glass we would see further oscillations.

Actually, if we plot the overlaps constructed from normalized wave functions, i.e.  $\langle \phi_n^g | \phi_n^s \rangle / (|\phi_n^g| \cdot |\phi_n^s|)$ , we are able to see three or four zeros. In fig. 3 this is illustrated for two cases, viz. two and six particles. A similar, very regular, behaviour is also displayed by the other particle numbers, except zero and fourteen, of course. It is worth noting, though, that these zeros do not at all coincide with the zeros of the interaction, which is obvious after what have been said above. Further, the peak values of these normalized overlaps increase with  $\lambda$ .

For all particle numbers ( $n$ ) we have calculated

$$V_n^P(\lambda, \omega_c) = \langle \phi_n^g(\lambda, \omega_c) | H' | \phi_n^s(\lambda, \omega_c) \rangle$$

where  $H' = H + \Delta(P^\dagger + P) - GP^\dagger P$ . This quantity represents the interaction matrix element after particle number projection. From the results of figs. 2 and 3 one should expect  $V_n^P(\lambda, \omega_c)$  to be an oscillating function of  $\lambda$ , and indeed so it is. It behaves rather irregular and displays only roughly the character of fig. 2. If we look at  $V_n^P(\lambda_n, \omega_c)$ , where  $\lambda_n$  corresponds to the  $n$ -particle peak value of fig. 1, we do not get a monotonic behaviour. Instead we get a relatively large value for  $n=2$ , a small value for  $n=4$ , a large value for  $n=6$ , a very small value for  $n=8$  and a very large value for  $n=10$ . This additional structure originates from the interference between  $\langle H_{sp} \rangle$  and  $G\langle P^\dagger P \rangle$  which both behave like in fig. 2. The rotation term,  $\langle \omega_j \chi \rangle$ , is still, however, rather small. Whether we can ascribe any physical significans to this is still an open question, which will be further discussed in a forthcoming publication [12].

We summarize:

- The constitution of the interaction matrix element between the 0 qp and the first excited 2 qp configuration is strongly dependent on how the non-interacting configurations are defined. With a natural definition we find that  $H_{sp}$  has the largest matrix elements while  $\omega_j \chi$  has very small values.
- If we resolve the wave functions of the g- and s-configurations into the constituents having definite particle number and calculate the overlap functions between these, we can understand the changes of sign from the relative phases that appear.

- A definite even particle number can be assigned to each interaction peak.
- Also after number projection the interaction oscillates. These oscillations, which depend on how the particles are distributed over the levels, will be scrutinized in a forthcoming publication [12].
- Two extremes can be distinguished, the  $\Delta=0$  limit and the  $H_{sp}=0$  limit. In none of these situations the oscillations of the interaction strength between the g- and s-configurations appear. Consequently all terms of the Hamiltonian are required in order to produce this behaviour.

Enlightening discussions with C.G. Andersson, R. Bengtsson, J. Krumlinde and B.R. Motteison are gratefully acknowledged. Thanks are due to Ingemar Ragnarsson for valuable comments on the manuscript.

## References

- [1] A.L. Goodman, *Advances in Nuclear Physics*, ed. J. Negele and E. Vogt, vol. 11 (Plenum Press, New York, 1979).
- [2] A. Faessler, M. Ploszajczak and K.W. Schmid, preprint, Tübingen 1980.
- [3] I. Hamamoto, *Nucl. Phys.* A271 (1976) 15.
- [4] E.R. Marshalek and A.L. Goodman, *Nucl. Phys.* A294 (1978) 92.
- [5] R. Bengtsson, I. Hamamoto and B. Mottelson, *Phys. Lett.* 73B (1978) 259.
- [6] J. Altmberger, I. Hamamoto and G. Leander, *Phys. Lett.* 80B (1979) 153;
- [7] F. Grümmer, K.W. Schmid and A. Faessler, *Nucl. Phys.* A326 (1979) 1.
- [8] R. Bengtsson and H.-B. Håkansson, preprint Lund 1980, to be published.
- [9] R. Bengtsson and S. Frauendorf, *Nucl. Phys.* A327 (1979) 139.
- [10] C.G. Andersson and J. Krumlind, *Nucl. Phys.* A334 (1980) 486.
- [11] C. Bloch and A. Messiah, *Nucl. Phys.* 39 (1962) 95.
- [12] R. Bengtsson and H.-B. Håkansson, current work, to be published.
- [13] F. Grümmer, K.W. Schmid and A. Faessler, *Nucl. Phys.* A308 (1978) 77.

### Figure captions

Fig. 1. The upper part shows the matrix elements between the non-interacting configurations as they are defined in the text. The solid line marked  $\omega_c/\omega_0$  gives the crossing frequency as a function of  $\lambda$ , while the curves marked N show the expectation values of the particle numbers for both configurations before the interaction is eliminated and at the frequency  $\omega_c$ . These curves are discontinuous and interchange character five times approximately halfway between the intersections [13]. At the very top of the diagram the single-particle energies are depicted for all seven  $i_{13/2}$ -levels. The lower part shows the fraction of the different particle numbers in the g-configuration (solid) and the s-configuration (dashed) as a function of  $\lambda(\omega_c)$ .

Fig. 2. The solid curves show the overlap functions  $\langle \phi_n^g | \phi_n^s \rangle$  for the different particle numbers (n) as a function of  $\lambda$ . The projected wave functions  $\phi_n^g$  and  $\phi_n^s$  have norms corresponding to the fractions in the original unprojected wave function. The dashed curves illustrate the matrix elements of  $GP^\dagger P$  in the 6 particle case and  $H_{sp}$  in the 8 particle case. If we choose  $G=0.125 \mu\omega_0$ , which is larger than the self-consistent value corresponding to  $\Delta=0.12 \mu\omega_0$  [8] but still realistic in a full scale calculation, we get the proportion between  $\langle H_{sp} \rangle$  and  $\langle GP^\dagger P \rangle$  as shown in the figure. As a rule the magnitudes increase with the particle number.

Fig. 3. Same as fig. 2 but for the absolute values of the normalized overlaps for two and six particles.

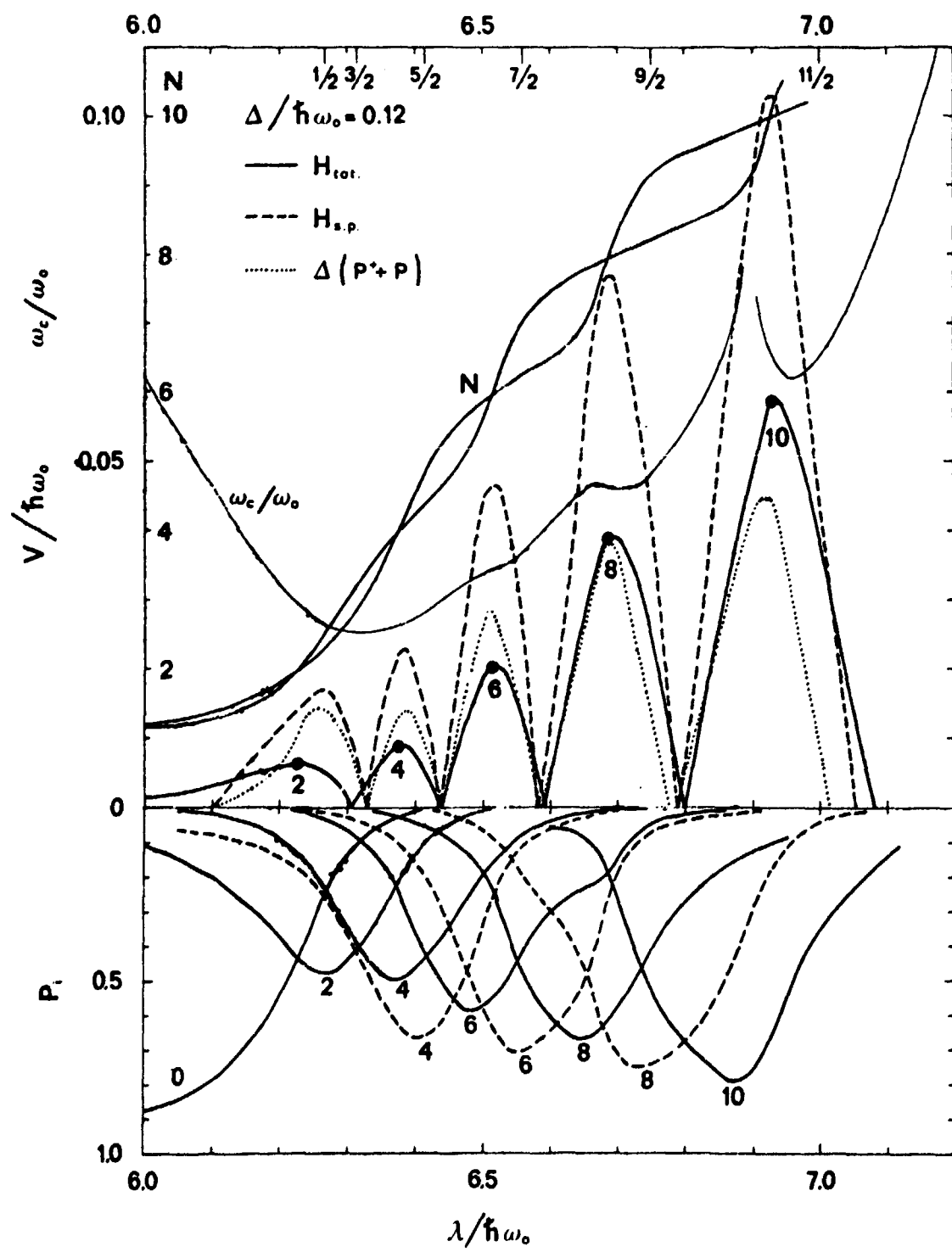
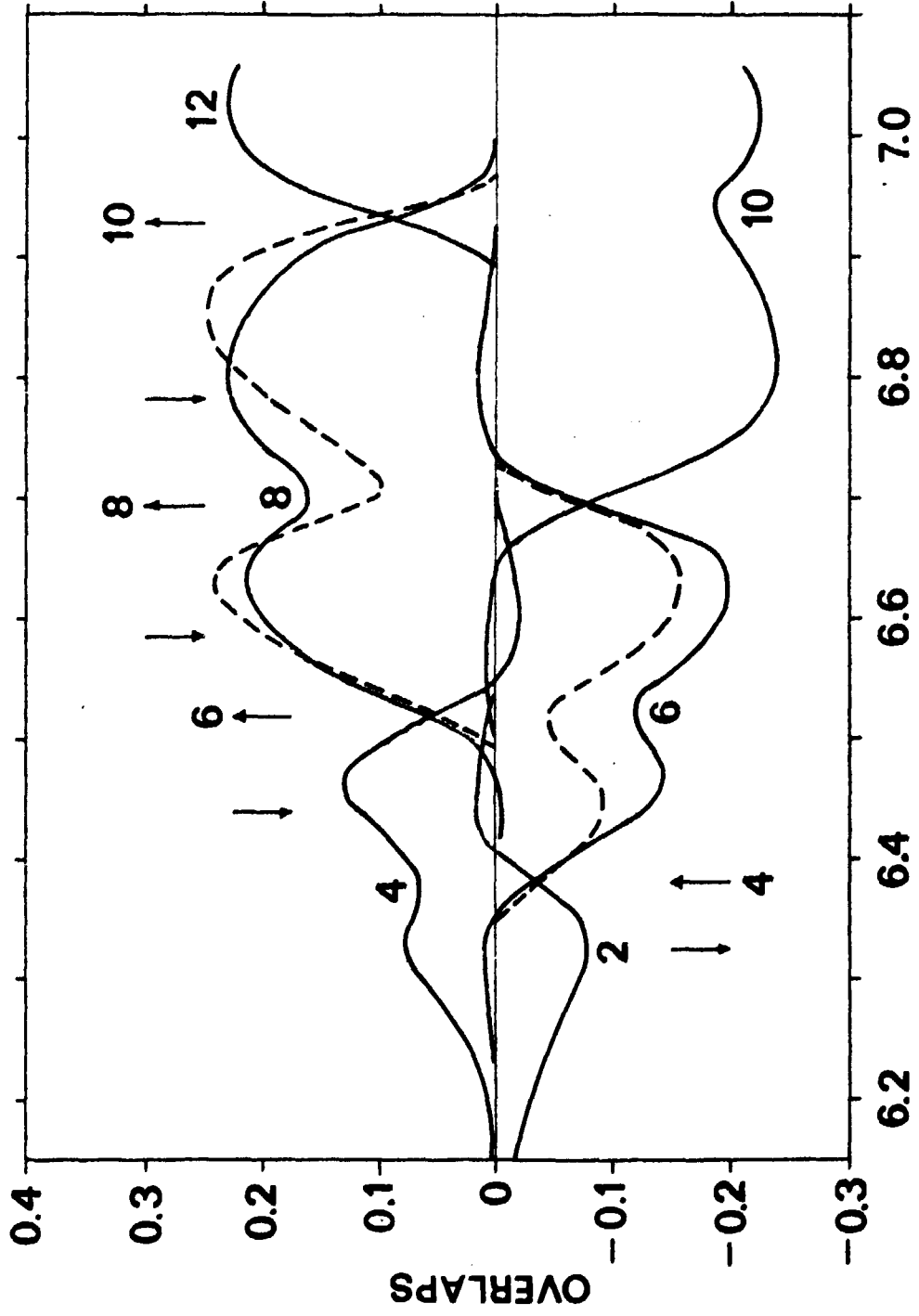


FIG. 1



$\lambda/h\omega_0$

FIG. 2

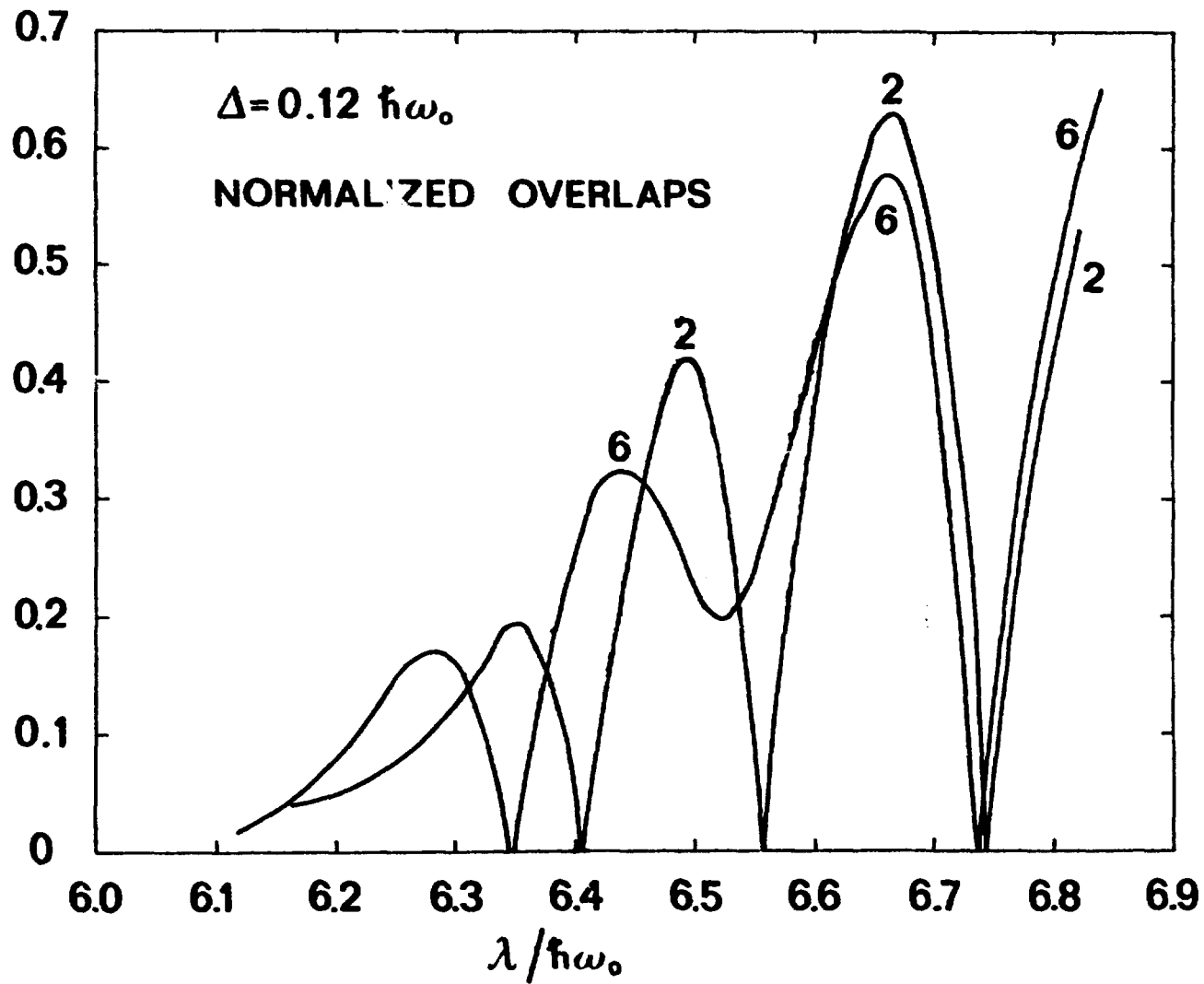


FIG. 3